Spin Liquid State in the S=1/2 Triangular Lattice Ba_{3}CuSb_{2}O_{9}

H. D. Zhou, E. S. Choi, G. Li, L. Balicas, C. R. Wiebe, Y. Qiu, J. R. D. Copley, and J. S. Gardner

Phys. Rev. Lett. **106**, 147204 — Published 6 April 2011

DOI: 10.1103/PhysRevLett.106.147204

Spin liquid state in the S = 1/2 triangular lattice $Ba_3CuSb_2O_9$

H. D. Zhou,[1,*] E. S. Choi,[1] G. Li,[1] L. Balicas,[1] C. R. Wiebe,[1,2,3] Y. Qiu,[4,5] J. R. D. Copley,[4] and J. S. Gardner[4,6]

[1]*National High Magnetic Field Laboratory, Florida State University, Tallahassee, FL 32306-4005, USA*
[2]*Department of Chemistry, University of Winnipeg, Winnipeg, MB, R3B 2E9 Canada*
[3]*Department of Chemistry, University of Manitoba, Winnipeg, MB, R3T 2N2 Canada*
[4]*NIST Center for Neutron Research, Gaithersburg, Maryland, 20899-6102, USA*
[5]*Department of Materials Science and Engineering, University of Maryland, College Park, Maryland, 20742, USA*
[6]*Indiana University, 2401 Milo B. Sampson Lane, Bloomington, Indiana 47408, USA*

The synthesis and characterization of $Ba_3CuSb_2O_9$, which has a layered array of Cu^{2+} spins in a triangular lattice, are reported. The magnetic susceptibility and neutron scattering experiments of this material show no magnetic ordering down to 0.2 K with a θ_{CW} = -55 K. The magnetic specific heat reveals a T-linear dependence with a γ = 43.4 $mJK^{-2}mol^{-1}$ below 1.4 K. These observations suggest that $Ba_3CuSb_2O_9$ is a new quantum spin liquid candidate with a S = 1/2 triangular lattice.

PACS numbers: 75.40.Cx, 75.40.Gb, 75.45.+j, 78.70.Nx

One of the current thrusts of modern condensed matter science has been the realization of an important model compound known as the quantum spin liquid (QSL)[1, 2]. The existence of these materials, in which magnetic spins remain quantum disordered in the limit of zero Kelvin, underpins much of modern condensed matter theory. Previous studies have shown that QSL ground states tend to emerge in the geometrically frustrated materials, in which the interactions among the limited magnetic degrees of freedom lead to a strong enhancement of quantum fluctuations. For example, the organic salts κ-(BEDT-TTF)$_2$Cu$_2$(CN)$_3$[3, 4] and $Et_nMe_{4-n}Sb[Pd(DMIT)_2]_2$[5–7] with a S = 1/2 triangular lattice, and $ZnCu_3(OH)_6Cl_2$ with a S = 1/2 kagomé lattice[8, 9] are all QSL candidates. While the study of the QSL state in the organic compounds remains a hot topic, there are very few inorganic materials identified as model systems for QSL ground states. Many efforts to synthesize spin liquids on triangular lattices in inorganic materials have failed. In this letter, we unveil a new candidate for a spin liquid compound - $Ba_3CuSb_2O_9$ - in which Cu^{2+} species form a geometrically frustrated triangular lattice. The magnetic susceptibility and neutron scattering experiments on this material show no magnetic ordering down to 0.2 K despite moderately strong antiferromagnetic interactions with $J \sim 32$ K. The magnetic specific heat reveals a T-linear dependence with a γ = 43.4 $mJK^{-2}mol^{-1}$ below 1.4 K, suggesting that a Fermi surface forms at finite temperatures in this inorganic insulator. These behaviours fit the predicted signatures of a spin liquid ground state with low amounts of chemical disorder.

Polycrystalline $Ba_3CuSb_2O_9$ samples were prepared by a solid state reaction. Appropriate mixtures of $BaCO_3$, CuO and Sb_2O_5 were ground together, pressed into pellets, and then calcined in air at 1070 °C for several days. The crystal structure of this 6-H perovskite-related material with $a = b = 5.8090$ Å and $c = 14.3210$ Å can be

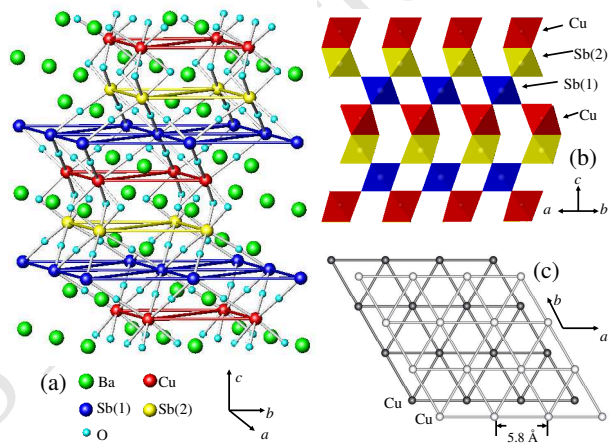

FIG. 1: (Color) (a) Schematic crystal structure for $Ba_3CuSb_2O_9$; (b) The layer structure along the c-axis; (c) The triangular lattice of Cu^{2+} in the ab plane.

represented as a framework consisting of corner-sharing SbO_6 octahedra and face-sharing $CuSbO_9$ bi-octahedra, as shown in Fig. 1(a, b). In the bi-octahedra, the Cu and Sb cations are well-ordered[10]. The Cu ions occupy the 2b Wyckoff site of space group $P6_3mc$, and this site forms the triangular lattice in the ab plane (Fig. 1(c)). Therefore, the structure can be seen as a two-dimensional triangular magnet, i.e., the Cu magnetic triangular lattices are magnetically separated by the two non-magnetic Sb layers (Fig. 1(b)). The powder x-ray diffraction (XRD) data of the as-prepared sample shows a single phase and no chemical disorder between Cu and Sb down to the few percentage level. The distance between two Cu ions in one triangle from the XRD refinement is uniformly 5.809(1) Å.

The temperature dependence of the DC magnetic susceptibility measured with μ_0H = 0.5 T for $Ba_3CuSb_2O_9$

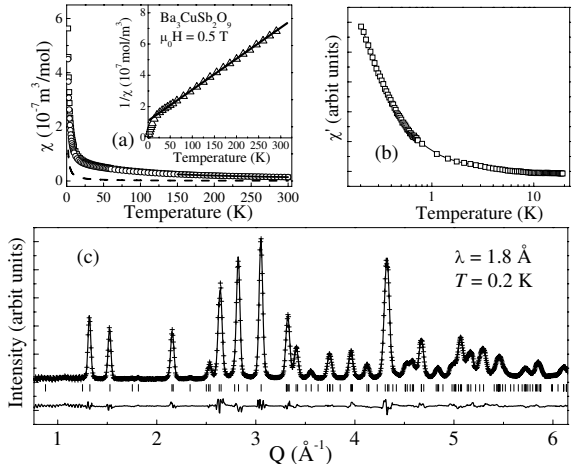

FIG. 2: (a) The temperature dependencies of the DC magnetic susceptibility (χ). The open squares, dash line, and open circles represent χ-as measured, χ-orphan spins, and χ-after deleting orphan spins, respectively. The solid curve on χ data above 150 K represents a fit to the HTSE. Inset: $1/\chi$-after deleting the orphan spin contribution (open triangles). The solid line on the $1/\chi$ data represents a Curie-Weiss fit. (b) The temperature dependence of the real part of the AC magnetic susceptibility (χ'). (c) Neutron diffraction pattern (crosses) for $Ba_3CuSb_2O_9$ at 0.2 K. The solid curve is the best fit from the Rietveld refinement using FullProf. The vertical marks indicate the position of Bragg peaks, and the bottom curve shows the difference between the observed and calculated intensities.

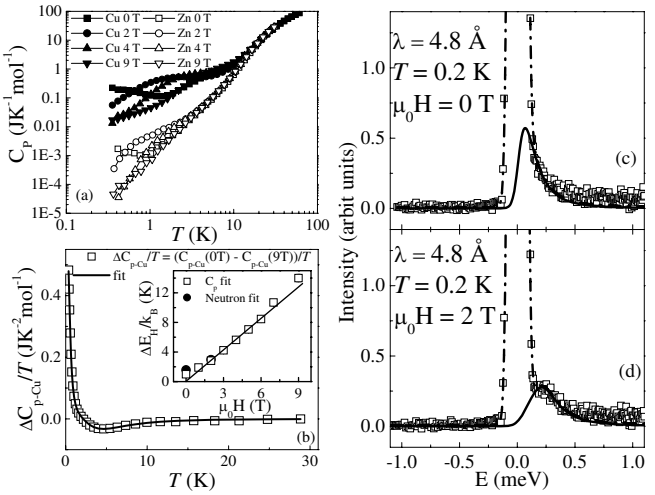

FIG. 3: (a) The temperature dependencies of specific heat at different fields for $Ba_3CuSb_2O_9$ and $Ba_3ZnSb_2O_9$. (b) open squares are $\Delta C_{P\text{-}Cu}/T = [C_{P\text{-}Cu}(0\ T)\text{-}C_{P\text{-}Cu}(9\ T)]/T$. The solid line is a fit as described in the text. Inset: ΔE_H as a function of $\mu_0 H$ between 0 and 9 T. The solid line represents a fit to Zeeman splitting. Inelastic neutron scattering spectra ($\lambda = 4.8$ Å) for $Ba_3CuSb_2O_9$ at 0.2 K with applied magnetic field 0 T (c) and 2 T (d). Open squares are experimental data, the dash-dot lines are the fits described in the text, the solid lines show the magnetic contribution.

shows no signature for a magnetic transition above 1.8 K, as indicated in Fig. 2(a). The temperature dependence of the AC magnetic susceptibility (Fig. 2(b)) further shows no sign of a magnetic transition down to 0.2 K. The neutron powder diffraction pattern obtained at 0.2 K with $\lambda = 1.8$ Å on the DCS at NIST (Fig. 2(c)) shows no intensity change nor additional peaks from the 4 K data (not shown here), indicating that there is no magnetic transition nor structural distortion down to 0.2 K. This is consistent with the AC susceptibility measurements. The possibility of mixing between the Cu and Sb sites has been tested by refinement of the neutron diffraction data. The best refinement (Fig. 2(c), using FullProf with $R_p \approx 5.0$, $R_{wp} \approx 7.5$, and $\chi^2 \approx 1.2$) shows a full occupancy of Sb(1) on the corner-sharing SbO_6 octahedron sites and Cu on one of the ordered bi-octahedra sites. There is a slight amount of site mixing (refined from the neutron data to be 5.1(4)%) of the other ordered bi-octahedra sites - Sb(2) sites are replaced by Cu ions. The DC magnetic susceptibility contribution from this 5.1% Cu^{2+} orphan spins has been calculated by a simple Curie law. The susceptibility, after subtracting this contribution, is shown as open circles in Fig. 2(a). Its inverse (inset of Fig. 2(a)) deviates from a linear temperature dependence around 30 K. The Curie-Weiss fit of this linear behaviour at high temperature gives a θ_{CW} = -55 K and an effective moment $\mu_{eff} = 1.79\ \mu_B$/Cu, which is consistent with the expected value for Cu^{2+} (S = 1/2) ions. This μ_{eff} gives a Lande g-factor g = 2.07 (again typical for Cu^{2+} (S = 1/2) ions). Using this g value, the exchange interaction J is estimated to be $J/k_B = 32$ K by fitting the data between 150 and 300 K to the calculation for the spin 1/2 triangular lattice using a high-temperature-series expansion (HTSE)[11]. As a consistency check, another method was used to calculate J based on mean-field theory, considering only z nearest-neighbour ions coupled with exchange interactions. θ_{CW} is given as $(-zJS(S+1))/3k_B$ (the Hamiltonian of the Heisenberg model here is $J\sum_{<i,j>} S_i \cdot S_j$). For the S =1/2 triangular lattice with $z = 6$, $J/k_B = -2/3\theta_{CW}$ = 37 K, which is consistent with the HTSE calculation.

Fig. 3(a) shows the specific heat (C_P) measured with a Physical Property Measurement System at different fields for $Ba_3CuSb_2O_9$ and the non-magnetic isostructural lattice standard $Ba_3ZnSb_2O_9$. The field-dependent specific heat at low temperatures for the non-magnetic $Ba_3ZnSb_2O_9$ sample is due to a nuclear Schottky anomaly from the Sb atoms[12], which is estimated to be of the order $10^{-5} \sim 10^{-3}$ $JK^{-1}mol^{-1}$. C_P of $Ba_3CuSb_2O_9$ also shows a field-dependent behaviour at low temperatures; the shoulder of C_P gradually moves to higher temperatures with increasing field. This anomaly is around $10^{-2} \sim 10^{0}$ $JK^{-1}mol^{-1}$, which apparently is

not due to the nuclear contribution from Sb. On the other hand, the 5.1% of Cu^{2+} ions on the Sb(2) sites could give rise to such a Schottky anomaly, which also has been found for the Cu^{2+} orphan spins in the spin liquid candidate $ZnCu_3(OH)_6Cl_2$ with Cu^{2+} kagome lattice[13]. Therefore, C_P for $Ba_3CuSb_2O_9$ includes four contributions: the lattice, the Sb Schottky anomaly, the Cu^{2+} orphan spins Schottky anomaly ($C_{Sch\text{-}orp.}$), and the magnetic specific heat for the Cu^{2+} triangular lattice (C_M). The lattice and Sb contributions are deleted by subtracting C_P of the $Ba_3ZnSb_2O_9$ sample. The remaining specific heat is $C_{P\text{-}Cu} = C_M + C_{Sch\text{-}orp.}$. To separate $C_{Sch\text{-}orp.}$, we have applied a similar analysis as described for the Schottky anomaly arising from the Cu^{2+} orphan spins in $ZnCu_3(OH)_6Cl_2$[13] and defects in Zn-doped Y_2BaNiO_5[14]. The difference was taken between the interpolated $C_{P\text{-}Cu}$ curves measured at different fields. Fig. 3(b) shows the difference between the 0 and 9 T curves $\Delta C_{P\text{-}Cu}/T = [C_{P\text{-}Cu}(0\ T)\text{-}C_{P\text{-}Cu}(9\ T)]/T$. This field-dependent part can be modeled by a dilute uniform distribution of zero-field split doublets, i.e. $S = 1/2$ spins. $\Delta C_{P\text{-}Cu}/T$ was fitted with $f[C(\Delta E_{H1})\ \text{-}\ C(\Delta E_{H2})]/T$, where f is the fraction of doublets per unit cell (or the percentage of the Cu^{2+} orphan spins) and $C(\Delta E_{H1})$ and $C(\Delta E_{H2})$ are the Schottky anomalies from a $S = 1/2$ spin with level splittings ΔE_{H1} and ΔE_{H2} by applying magnetic fields H1 and H2, respectively. The best fit, as the solid line shown in Fig. 3(b), results in $f = 4.8(2)\%$. This amount of the Cu^{2+} orphan spins is consistent with the amount obtained from the refinement of the neutron diffraction data. The obtained ΔE_H is plotted in the inset of Fig. 3(b). The linear fitting of ΔE_H with $\mu_0 H \geq 1$ T results in a Zeeman splitting with $g \approx 2.1$. The zero-field splitting of the doublets is 0.98 K(0.089 meV).

These orphan spins have a characteristic inelastic neutron scattering signature - namely, a Zeeman-like splitting under applied fields. Fig. 3(c,d) shows the inelastic neutron scattering spectra for $Ba_3CuSb_2O_9$ at 0.2 K with $\mu_0 H = 0$ and 2 T. A small quasi-static component is readily visible in the data, with a shoulder extending to higher energies developing with increasing field. The spectra, after correcting with a resolution-convolution, can be fit as:

$$I(E) = A\delta(E) + B(n(E)+1)\frac{E\Delta E_H \Gamma}{(E^2 - \Delta E_H^2)^2 + E^2\Gamma^2} \quad (1)$$

where the first Dirac term represents the incoherent nuclear scattering and the second damped simple harmonic oscillator term represents the quasi-static component (A and B are proportionality coefficients). $n(E)$ is the Bose factor and Γ is the damping. The fitting parameters are $\Delta E_H = 0.144$ meV, $\Gamma = 0.316$ for 0 T data, and $\Delta E_H = 0.27$ meV, $\Gamma = 0.36$ for 2 T data. In Fig. 3(c,d), the fits of the quasi-static component are shown as solid lines. The values of the ΔE_H obtained here are consistent with the energy splitting obtained from the specific heat analysis, as shown in the inset of Fig. 3(b), which indicates that the excitations observed are due to orphan spins.

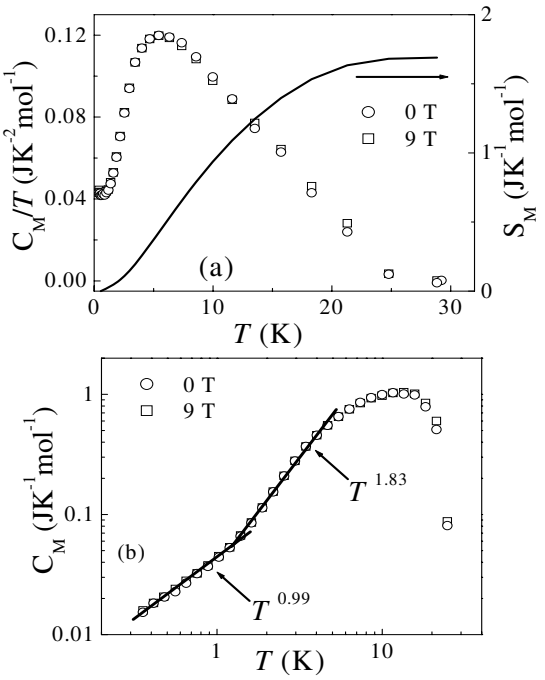

FIG. 4: (a) The temperature dependencies of C_M/T and the magnetic entropy variation S_M; (b) The temperature dependence of C_M (open symbols). The solid lines are fits as described in the text.

The magnetic specific heat (C_M) of the Cu^{2+} triangular lattice is finally obtained by subtracting $C_{Sch\text{-}orp.} = fC(\Delta E_H)$. The result for the data is shown in Figure 4. Several features are noteworthy: (i) C_M shows no field-dependence with $\mu_0 H \leq 9$ T. (ii) The magnetic contribution of the specific heat becomes prominent at around 30 K, which is where the magnetic susceptibility also deviates from the Curie-Weiss behaviour. (iii) C_M/T shows a broad peak around 5 K and becomes flat below 1.4 K (Fig. 4(a)). (iv) The integrated magnetic entropy variation below 30 K is 1.7 $JK^{-1}mol^{-1}$, which is around 30% of $R\ln(2)$ for $S = 1/2$ system, where R is the gas constant. This feature indicates a high degeneracy of low-energy states at low temperatures. (v) As shown in Fig. 4(b) with the log-log scale, between 1.4 and 4 K, C_M can be fit as $C_M = bT^\alpha$ with b = 37.0 $mJK^{-3}mol^{-1}$ and $\alpha = 1.83(2)$. This α value is near 2.0, showing a quadratic temperature dependence. At lower temperatures, between 0.35 and 1.4 K, C_M can be fit as $C_M = \gamma T^\alpha$ with $\gamma = 43.4$ $mJK^{-2}mol^{-1}$ and $\alpha = 0.99(2)$, giving a linear temperature dependence.

The susceptibility and specific heat both show no magnetic ordering down to 0.2 K for $Ba_3CuSb_2O_9$ despite

moderately strong nearest neighbour antiferromagnetic interactions with $J \sim 32$ K, which clearly places this compound in the highly frustrated regime. The field-independent C_M is common in spin liquid candidates, which should be resilient to moderate applied fields. This behaviour has also been observed for other spin liquid candidates, such as $NiGa_2S_4$ with Ni^{2+} (S = 1) triangular lattice[15] and $Na_4Ir_3O_8$ with Ir^{4+} (S = 1/2) hyper-kagome lattice[16]. On the other hand, the linear dependence of C_M is unusual for 2D frustrated lattices, which should have a quadratic dependence for linearly dispersive low energy modes. However a linear-T dependence has been predicted by the resonating-valence-bond (RVB) model of Anderson at low temperatures, due to the pairing of spins into singlets[17]. For example, the studied organic quantum spin liquid (QSL) candidate κ-(BEDT-TTF)$_2$Cu$_2$(CN)$_3$ with Cu^{2+} triangular lattice also shows $C \propto \gamma T$ with $\gamma = 12$ mJK^{-2}mol^{-1} of Cu^{2+}[3]. $Ba_3CuSb_2O_9$ has a larger $\gamma = 43.4$ mJK^{-2}mol^{-1}. The origin of this linear specific heat term, however, is still a matter of debate by theorists. One current mode of thought is that a Fermi surface of excitations is formed within the liquid state, which gives rise to a linear term even for Mott insulators such as $Ba_3CuSb_2O_9$. Lee *et al.*, for example, have proposed an instability of a Fermi surface of spinons in the long-ranged RVB state to explain the experimental results of κ-(BEDT-TTF)$_2$Cu$_2$(CN)$_3$[18]. Related theories also have been proposed for $ZnCu_3(OH)_6Cl_2$[19] and $Na_4Ir_3O_8$[20]. One experimental prediction of Lee's theory, however, is that a spontaneous breaking of lattice symmetry occurs in the liquid state, but no obvious structural distortion has been observed for $Ba_3CuSb_2O_9$ in this study. These distortions, however, can be exceedingly small and difficult to detect by conventional scattering techniques. Combining the magnetism and specific heat, the evolution of the spin dynamics of $Ba_3CuSb_2O_9$ with decreasing temperature can be described as: (i) by 30 K, there is a build-up of spin fluctuations; (ii) by around 5 K, well below the magnetic interaction energy scale ~ 30 K, the system enters a spin liquid ground state whose dynamics has quantum character.

The change of exponent (α) for the low temperature specific heat has also been observed for the kagome system $ZnCu_3(OH)_6Cl_2$. In $ZnCu_3(OH)_6Cl_2$, α changes from 1.7 to 1.3 with decreasing temperature[13]. Although the value of α could have a substantial experimental error due to the lack of a proper lattice standard for $ZnCu_3(OH)_6Cl_2$, the change of α could also be an indication for the appearance of a QSL state as discussed above for $Ba_3CuSb_2O_9$. The Cu^{2+} orphan spins sitting on the Sb(2) sites for $Ba_3CuSb_2O_9$ act as doublets, which is also similar to the behaviour of the Cu^{2+} spins sitting on the Zn sites for $ZnCu_3(OH)_6Cl_2$[9, 13]. The zero-field splitting of the doublets shows that the splitting is due to a coupling with the liquid state, not a paramagnetic impurity phase - the Cu^{2+} orphan spins on Sb(2) sites are weakly coupled to the spin liquid states of Cu^{2+} spins on the triangular lattice.

At last, we point out that $Ba_3CuSb_2O_9$ is an excellent model spin liquid due to the clear method of obtaining a non-magnetic lattice standard (and thus the magnetic specific heat contribution), and it is a relatively clean example of QSL behaviour in an inorganic oxide. Future experiments, preferably on single crystals, will be able to answer more fundamental questions about this compound, including the nature of the excitation spectrum (fermionic or bosonic), the possibility of the emergence of new phases under doping (such as the closely related superconducting states in the charge transfer salts), and the true ground state down to temperatures less than 0.2 K[21, 22].

This work is supported by NSF-DMR-0654118 and the State of Florida. C. R. W. is grateful for support through NSERC of Canada. The neutron work utilized facilities supported in part by the National Science Foundation under Agreement No. DMR-0454672.

* Electronic address: zhou@magnet.fsu.edu

[1] L. Balents, Nature **464**, 199 (2010).
[2] R. Moessner and A. P. Ramirez, Physics Today **59**, 24 (2006).
[3] S. Yamashita *et al.*, Nature Phys. **4**, 459 (2008).
[4] M. Yamashita *et al.*, Nature Phys. **5**, 44 (2009).
[5] M. Yamashita *et al.*, Science **328**, 1246 (2010).
[6] T. Itou *et al.*, Nature Phys. DOI:10.1038/nphys1715.
[7] T. Itou *et al.*, J. Phys. Condens. Matter **19**, 145247 (2007).
[8] J. S. Helton *et al.*, Phys. Rev. Lett. **98**, 107204 (2007).
[9] S. H. Lee *et al.*, Nature Mater. **6**, 853 (2007).
[10] Von. P. Köhl *et al.*, Z. Anorg. Allg. Chem. **422**, 280 (1978).
[11] H. E. Stanley, Phys. Rev. **158**, 546 (1967).
[12] H. K. Collan *et al.*, Phys. Rev. B **1**, 2888 (1967).
[13] M. A. De Vries *et al.*, Phys. Rev. Lett. **100**, 157205 (2008).
[14] A. P. Ramirez *et al.*, Phys. Rev. Lett. **72**, 3108 (1994).
[15] S. Nakatsuji *et al.*, Science **309**, 1697 (2005).
[16] Y. Okamoto *et al.*, Phys. Rev. Lett. **99**, 137207 (2007).
[17] P. W. Anderson, Science **235**, 1196 (1987).
[18] S. S. Lee *et al.*, Phys. Rev. Lett. **98**, 067006 (2007).
[19] Y. Ran *et al.*, Phys. Rev. Lett. **98**, 117205 (2007).
[20] M. J. Lawler *et al.*, Phys. Rev. Lett. **101**, 197202 (2008).
[21] B. J. Powell and R. H. McKenzie, R. H. arXiv:1007.5381 (2010).
[22] P. A. Lee *et al.*, Reviews of Modern Physics **78**, 17-85 (2006).